Mineralogical Magazine (2021), **85**, 772–783
doi:10.1180/mgm.2021.64

CAMBRIDGE UNIVERSITY PRESS

Article

The mineralogy of the historical Mochalin Log *REE* deposit, South Urals, Russia. Part IV. Alexkuznetsovite-(La), $La_2Mn(CO_3)(Si_2O_7)$, alexkuznetsovite-(Ce), $Ce_2Mn(CO_3)(Si_2O_7)$ and biraite-(La), $La_2Fe^{2+}(CO_3)(Si_2O_7)$, three new isostructural minerals and a definition of the biraite group

Anatoly V. Kasatkin[1]*, Natalia V. Zubkova[2], Igor V. Pekov[2,3], Nikita V. Chukanov[4], Radek Škoda[5], Atali A. Agakhanov[1], Dmitriy I. Belakovskiy[1], Sergey N. Britvin[6] and Dmitry Yu. Pushcharovsky[2]

[1]Fersman Mineralogical Museum of the Russian Academy of Sciences, Leninsky Prospekt 18-2, 119071 Moscow, Russia; [2]Faculty of Geology, Moscow State University, Vorobievy Gory, 119991 Moscow, Russia; [3]Vernadsky Institute of Geochemistry and Analytical Chemistry, Russian Academy of Sciences, Kosygina str. 19, 119991 Moscow, Russia; [4]Institute of Problems of Chemical Physics, Russian Academy of Sciences, 142432 Chernogolovka, Moscow region, Russia; [5]Department of Geological Sciences, Faculty of Science, Masaryk University, Kotlářská 2, 611 37, Brno, Czech Republic; and [6]Institute of Earth Sciences, St Petersburg State University, University Embankment 7/9, 199034 St Petersburg, Russia

Abstract

Three new isostructural minerals, alexkuznetsovite-(La), ideally $La_2Mn(CO_3)(Si_2O_7)$, alexkuznetsovite-(Ce) $Ce_2Mn(CO_3)(Si_2O_7)$ and biraite-(La) $La_2Fe^{2+}(CO_3)(Si_2O_7)$, were discovered in polymineralic nodules from the Mochalin Log *REE* deposit, South Urals, Russia. The new minerals form anhedral grains up to 0.3 mm × 0.4 mm [alexkuznetsovite-(La)], 0.5 mm × 0.9 mm [alexkuznetsovite-(Ce)] and 0.2 mm × 1.2 mm [biraite-(La)] embedded in granular aggregates consisting of different *REE* minerals [allanite-(Ce)/-(La), bastnäsite-(Ce)/-(La), fluorbritholite-(Ce), perbøeite-(Ce)/-(La), percleveite-(Ce)/-(La) and törnebohmite-(Ce)/-(La)]. All three new species are brown to dark brown, translucent in thin fragments, with white streak, vitreous lustre and Mohs' hardness of ~5. D_{calc} = 4.713 [alexkuznetsovite-(La)], 4.687 [alexkuznetsovite-(Ce)] and 4.682 [biraite-La)] g·cm^{-3}. Their empirical formulae, calculated on the basis of 2 Si and 10 O apfu, are: alexkuznetsovite-(La): $(La_{0.98}Ce_{0.89}Nd_{0.10}Pr_{0.05})_{\Sigma 2.02}Mn^{2+}_{0.50}Fe^{2+}_{0.29}Ca_{0.12}Mg_{0.03}(CO_3)_{0.94}(HCO_3)_{0.06}(Si_2O_7)$; alexkuznetsovite-(Ce): $(Ce_{0.96}La_{0.78}Nd_{0.16}Pr_{0.07})_{\Sigma 1.97}Th_{0.01}Mn^{2+}_{0.50}Fe^{2+}_{0.33}Ca_{0.14}Mg_{0.02}(CO_3)_{0.93}(HCO_3)_{0.07}(Si_2O_7)$; and biraite-(La): $(La_{0.95}Ce_{0.87}Nd_{0.08}Pr_{0.04})_{\Sigma 1.94}Th_{0.01}Ca_{0.12}Fe^{2+}_{0.44}Mn^{2+}_{0.38}Mg_{0.07}(CO_3)_{0.88}(HCO_3)_{0.12}(Si_2O_7)$. The new minerals are monoclinic, $P2_1/c$ and Z = 4. The unit-cell parameters of alexkuznetsovite-(La)/alexkuznetsovite-(Ce)/biraite-(La) are: a = 6.5642(3)/6.5764(4)/6.5660(10), b = 6.7689(3)/6.7685(4)/6.7666(11), c = 18.7213(10)/18.7493(15)/18.698(3) Å, β = 108.684(6)/108.672(8)/108.952(16)° and V = 788.00(7)/790.66(10)/785.7(2) Å^3. The crystal structures are solved from single-crystal X-ray diffraction data; R = 0.0628 [alexkuznetsovite-(La)], 0.0589 [alexkuznetsovite-(Ce)] and 0.1193 [biraite-(La)]. A new biraite group is defined; it includes isostructural biraite-(Ce) and the three new minerals described herein. The rootname alexkuznetsovite is given in honour of the Russian mineral collector Alexey M. Kuznetsov (born 1962) who provided samples in which all three new minerals were found. The Levinson's suffix-modifier -(La) or -(Ce) indicates the predominance of La or Ce among *REE* in the mineral. Biraite-(La) is named as an analogue of biraite-(Ce) with La prevailing among *REE*.

Keywords: alexkuznetsovite-(La), alexkuznetsovite-(Ce), biraite-(La), new mineral, rare-earth carbonate-silicate, crystal structure, biraite group, Mochalin Log, South Urals

(Received 1 June 2021; accepted 29 July 2021; Accepted Manuscript published online: 3 August 2021; Associate Editor: Mihoko Hoshino)

Introduction

This article continues a series of papers on the mineralogy and crystal chemistry of new mineral species containing rare earth elements (*REE*) as species-defining cations (henceforth '*REE* minerals') discovered by our team at the Mochalin Log deposit, Chelyabinsk Oblast, South Urals, Russia (55°48'42"N, 60°33'46"E). A brief outline of the history of studies, the general data on geology and mineralogy of this rare-earth deposit as well as the description of two new isostructural gatelite-group minerals, ferriperbøeite-(La) and perbøeite-(La) were given in the first paper of this series (Kasatkin *et al.*, 2020a). The second article reported on radekškodaite-(La) and radekškodaite-(Ce), two members of the epidote–törnebohmite polysomatic series with a novel-type structure including one epidote and two

***Author for correspondence:** Anatoly V. Kasatkin, Email: anatoly.kasatkin@gmail.com
Cite this article: Kasatkin A.V., Zubkova N.V., Pekov I.V., Chukanov N.V., Škoda R., Agakhanov A.A., Belakovskiy D.I., Britvin S.N. and Yu. Pushcharovsky D. (2021) The mineralogy of the historical Mochalin Log *REE* deposit, South Urals, Russia. Part IV. Alexkuznetsovite-(La), $La_2Mn(CO_3)(Si_2O_7)$, alexkuznetsovite-(Ce), $Ce_2Mn(CO_3)(Si_2O_7)$ and biraite-(La), $La_2Fe^{2+}(CO_3)(Si_2O_7)$, three new isostructural minerals and a definition of the biraite group. *Mineralogical Magazine* **85**, 772–783. https://doi.org/10.1180/mgm.2021.64

törnebohmite modules (ET2) (Kasatkin *et al.*, 2020b). The third paper contained data on the new mineral species percleveite-(La) (Kasatkin *et al.*, 2020c). Herein we describe another three *REE* minerals: alexkuznetsovite-(La) [Russian Cyrillic: алекскузнецовит-(La)], ideally $La_2Mn(CO_3)(Si_2O_7)$, alexkuznetsovite-(Ce) [Russian Cyrillic: алекскузнецовит-(Ce)], ideally $Ce_2Mn(CO_3)(Si_2O_7)$, and biraite-(La) [Russian Cyrillic: бираит-(La)], ideally $La_2Fe^{2+}(CO_3)(Si_2O_7)$. All three new species from Mochalin Log are isostructural to each other and to biraite-(Ce), described previously from the Biraya *REE*–Fe occurrence, Irkutsk Oblast, Siberia, Russia (Konev *et al.*, 2005). According to the principles for group nomenclature (Mills *et al.*, 2009), the biraite group, composed of the four minerals mentioned above, is established. Biraite-group members are monoclinic, $P2_1/c$, with the general formula expressed as $A_2M(CO_3)(Si_2O_7)$, where $A = \boldsymbol{REE}^{3+}$, Na, Ca, Ba, Th and vacancy, and $M = \mathbf{Fe}^{2+}$, $\mathbf{Mn}^{2+}$, Mg, Ca, Al, REE^{3+} and Ti (species-defining constituents are given in boldtype). Biraite and alexkuznetsovite are distinguished by the predominant cation at the *M* site. The *M* site is predominantly occupied by Fe^{2+} in the former and Mn^{2+} in the latter mineral.

Alexkuznetsovite-(La) [pronounced: a lex kuz ne tso vait], discovered prior to the two others, was named in honour of Alexey Mikhailovitch Kuznetsov (born 21.11.1962), a mineral collector and amateur mineralogist from Chelyabinsk, Russia. His extensive mineral collection is focused exclusively on the minerals of South Urals, most of which have been collected by himself during numerous field trips throughout the region. Specimens collected by Alexey Kuznetsov served as a base for numerous scientific studies and papers devoted to the mineralogy of the South Urals: see, e.g. Pekov *et al.* (2013), Belogub *et al.* (2015), Kolisnichenko *et al.* (2017) and Kasatkin *et al.* (2017, 2019a, 2019b). Five new *REE* minerals from the Mochalin Log deposit described in previous papers of the present series (Kasatkin *et al.*, 2020a,b,c) and the three new species characterised here have been discovered during the investigation of specimens from his collection. The Levinson's suffix-modifier -(La) in the mineral name reflects the predominance of La among *REE*. Alexkuznetsovite-(Ce) was named as an analogue of alexkuznetsovite-(La) with Ce predominant over each of the other *REE*. Biraite-(La) was named as an analogue of biraite-(Ce) (Konev *et al.*, 2005) with La predominance over other *REE*.

All three new minerals and their names have been approved by the International Mineralogical Association (IMA) Commission on New Minerals, Nomenclature and Classification (CNMNC): IMA2019–081 [alexkuznetsovite-(La), Kasatkin *et al.*, 2019c], IMA2019–118 [alexkuznetsovite-(Ce), Kasatkin *et al.*, 2020d] and IMA2020–020 [biraite-(La), Kasatkin *et al.*, 2020e]. The mineral symbol (Warr, 2021) for alexkuznetsovite-(La) and alexkuznetsovite-(Ce) is Alx-La and Alx-Ce, respectively, and biraite-(La) is Bir-La. The type specimens are deposited in the systematic collection of the Fersman Mineralogical Museum of the Russian Academy of Sciences, Moscow with the catalogue numbers: alexkuznetsovite-(La) – 97005 (holotype), 97024 and 97025 (parts of holotype); alexkuznetsovite-(Ce) – 97008 (holotype) and 97026 (cotype); biraite-(La) – 97023 (holotype).

Occurrence and general appearance

Polymineralic nodules containing the new minerals were found in the 1980s by local collectors at the historical dump no. 2 within the Mochalin Log valley and, since that time, deposited in the collection of Alexey M. Kuznetsov. In 2018 they were cut, polished and sent to the senior author for preliminary electron microprobe analysis (EMPA) that revealed three novel *REE*-bearing phases.

According to the distribution scale of *REE* minerals found at the Mochalin Log deposit (Kasatkin *et al.*, 2020a), all three minerals should be considered as rare. Among 300 nodules with *REE*-bearing minerals investigated by us, alexkuznetsovite-(La) was found in only eight nodules, alexkuznetsovite-(Ce) in 13 and biraite-(La) in nine of them. The first two of these minerals co-exist in seven nodules while all three species are found together in only one of them.

The new minerals occur in a very *REE*-rich mineral assemblage with dominant allanite-(Ce)/-(La), bastnäsite-(Ce)/-(La), fluorbritholite-(Ce), perbøeite-(Ce)/-(La), percleveite-(Ce)/-(La) and törnebohmite-(Ce)/-(La). Other *REE* minerals associated with all three new species include biraite-(Ce), ferriallanite-(Ce)/-(La), ferriperbøeite-(Ce)/-(La), perrierite-(Ce)/-(La) and monazite-(Ce)/-(La). Both alexkuznetsovite-(La) and biraite-(La) are also associated with radekškodaite-(La); alexkuznetsovite-(Ce) alone – with christofschäferite-(Ce), dissakisite-(Ce)/-(La), gatelite-(Ce)/-(La), hydroxylbastnäsite-(Ce), lanthanite-(La); and biraite-(La) alone – with ancylite-(La), *REE*-bearing epidote, stillwellite-(Ce) and stetindite-(Ce). Non-*REE* minerals present in the assemblage include hollandite, nontronite, microcline, pyrite, quartz, thorianite and thorite.

The new minerals form isolated anhedral grains up to 0.3 mm × 0.4 mm [alexkuznetsovite-(La)], 0.5 mm × 0.9 mm [alexkuznetsovite-(Ce)] and 0.2 mm × 1.2 mm [biraite-(La)] embedded in granular aggregates of other, above-listed *REE* minerals (Figs 1–3).

Physical properties and optical data

All three new species are brown to dark brown, translucent in thin fragments, have white streak and vitreous lustre. They are non-fluorescent under ultraviolet light. Neither cleavage nor parting are observed. The new minerals are brittle with an uneven fracture. Their Vickers' hardness values (load 150 g) are equal to 722 kg/mm^2 (range 657–787, $n = 5$) for alexkuznetsovite-(La), 745 kg/mm^2 (range 690–800, $n = 5$) for alexkuznetsovite-(Ce) and to 712 kg mm^{-2} (range 636–800, $n = 5$) for biraite-(La). All these values correspond to *ca.* 5 on the Mohs' scale. Density could not be measured due to lack of sufficiently large monomineralic fragments and the absence of heavy liquids with suitable density. Density values calculated using the empirical formulae and the unit-cell parameters from single-crystal XRD data are (g cm^{-3}): 4.713 for alexkuznetsovite-(La), 4.687 for alexkuznetsovite-(Ce) and 4.682 for biraite-(La).

In transmitted plane polarised light, the new minerals are light brown and non-pleochroic. Optically, they are biaxial (–). Alexkuznetsovite-(La) has $\alpha = 1.780(6)$, $\beta = 1.807(6)$, $\gamma = 1.818(6)$ (589 nm), $2V_{meas.} = 65(10)°$ and $2V_{calc.} = 64°$. Alexkuznetsovite-(Ce) has $\alpha = 1.790(6)$, $\beta = 1.812(6)$, $\gamma = 1.824(8)$ (589 nm), $2V_{meas.} = 70(10)°$ and $2V_{calc.} = 72°$. Biraite-(La) has $\alpha = 1.770(5)$, $\beta = 1.790(5)$, $\gamma = 1.800(5)$ (589 nm), $2V_{meas.} = 70(10)°$ and $2V_{calc.} = 70°$. The 2V values are estimated by the curvature degree of the isogyre on the sections perpendicular to the optical axes. In all three cases, dispersion of optical axes is weak, $r > v$. Optical orientation was not determined for any of the new minerals due to the anhedral shape of their grains.

The Gladstone-Dale compatibility index $(1 - K_p/K_c)$ is 0.005, –0.014 and 0.016 for alexkuznetsovite-(La), alexkuznetsovite-(Ce) and biraite-(La), respectively, using their empirical formulae and the unit-cell parameters determined from single-crystal XRD data. All the values are rated as superior (Mandarino, 1981).

The new minerals are soluble in concentrated hydrochloric and nitric acids with CO_2 evolution.

https://doi.org/10.1180/mgm.2021.64 Published online by Cambridge University Press

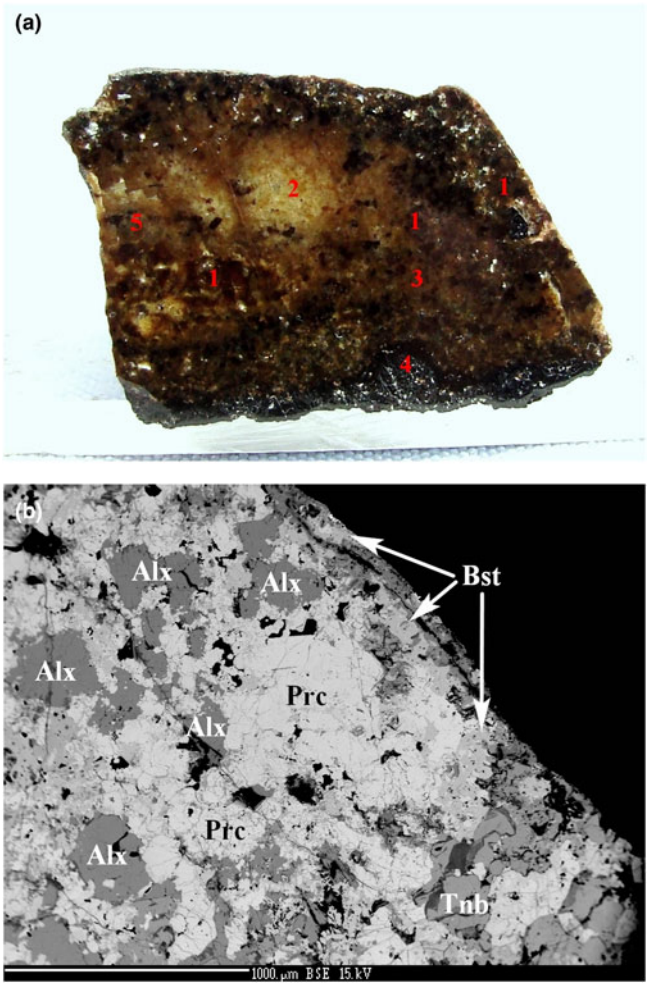

Fig. 1. (*a*) Polished section of nodule showing zones of: (1) dark brown alexkuznetsovite-(La) intergrown with (2) light yellow-brown percleveite-(La); (3) orange-brown bastnäsite-(La)/-(Ce) and fluorbritholite-(Ce); (4) black allanite-(La)/-(Ce) and perbøeite-(La)/-(Ce); and (5) greenish törnebohmite-(La). Size of sample: 1.6 cm × 2.3 cm, specimen no. ML 89-2. (*b*) Fragment of (*a*): alexkuznetsovite-(La) (Alx) associated with percleveite-(La) (Prc), törnebohmite-(La) (Tnb) and bastnäsite-(La) (Bst). Black grains are quartz. Polished section. SEM (back-scattered electron) image. Scale bar = 1 mm.

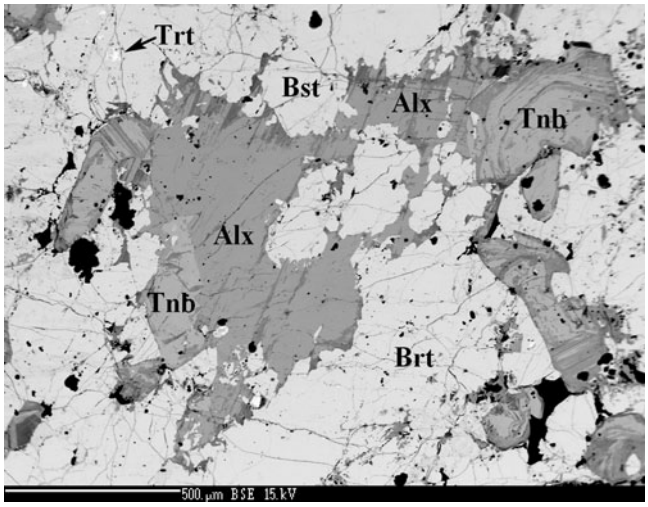

Fig. 2. Alexkuznetsovite-(Ce) (Alx) associated with törnebohmite-(La) (Tnb), fluorbritholite-(Ce) (Brt), bastnäsite-(Ce) (Bst) and thorite (Trt). Black grains are quartz. Specimen no. ML 88-2. Polished section. SEM (backscattered electron) image. Scale bar = 0.5 mm.

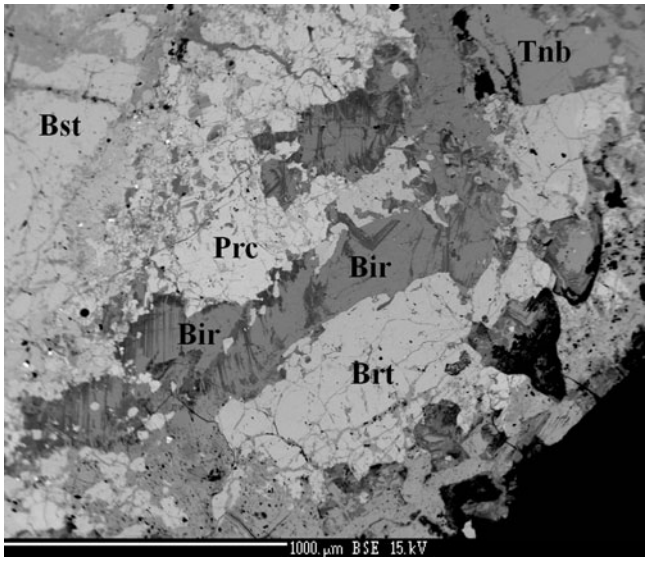

Fig. 3. Biraite-(La) (Bir) associated with törnebohmite-(La) (Tnb), fluorbritholite-(Ce) (Brt), percleveite-(Ce)/-(La) (Prc) and bastnäsite-(Ce) (Bst). Black grains are quartz. Specimen no. ML 79-2. Polished section. SEM (back-scattered electron) image. Scale bar = 1 mm.

Raman spectroscopy

The Raman spectra (Figs 4 and 5) of alexkuznetsovite-(La), alexkuznetsovite-(Ce) and biraite-(La) were obtained from polished sections by means of a Horiba Labram HR Evolution spectrometer. This dispersive, edge-filter-based system is equipped with an Olympus BX 41 optical microscope, a diffraction grating with 600 grooves per millimetre, and a Peltier-cooled, Si-based charge-coupled device (CCD) detector. After careful tests with different lasers (473, 532 and 633 nm), the 532 nm diode-based laser with the beam power of 20 mW at the sample surface was selected for spectra acquisition to minimise analytical artefacts. The Raman signal was collected in the range of 100–4000 cm^{-1} with a 50× objective and the system was operated in the confocal mode, beam diameter was ~2.6 μm and the depth resolution ~5 μm. No visual damage of the analysed surface was observed at these conditions after the excitation. Wavenumber calibration was done using the Rayleigh line and low-pressure Ne-lamp emissions. The wavenumber accuracy was ~0.5 cm^{-1}, and the spectral resolution was ~2 cm^{-1}. Band fitting was done after appropriate background correction, assuming combined Lorentzian-Gaussian band shapes using the Voigt function (*PeakFit*; Jandel Scientific Software).

The spectra of all three new minerals are similar, but Raman bands of alexkuznetsovite-(Ce) and biraite-(La) are broadened and less well resolved as compared to analogous bands of alexkuznetsovite-(La), which may be due to structural defects originated as a result of alpha-decay of admixed thorium (see Table 1) occurring in variable amounts.

The assignment of the Raman bands is as follows. The bands in the range of 1340–1560 cm^{-1} are due to doubly degenerate asymmetric C–O stretching vibrations of CO_3^{2-} anions (the ν_3 mode). These bands are Raman active because of a strong distortion of the CO_3 triangle (see below). Additional splitting may be due to Fermi resonance with the overtone of the band of in-plane

https://doi.org/10.1180/mgm.2021.64 Published online by Cambridge University Press

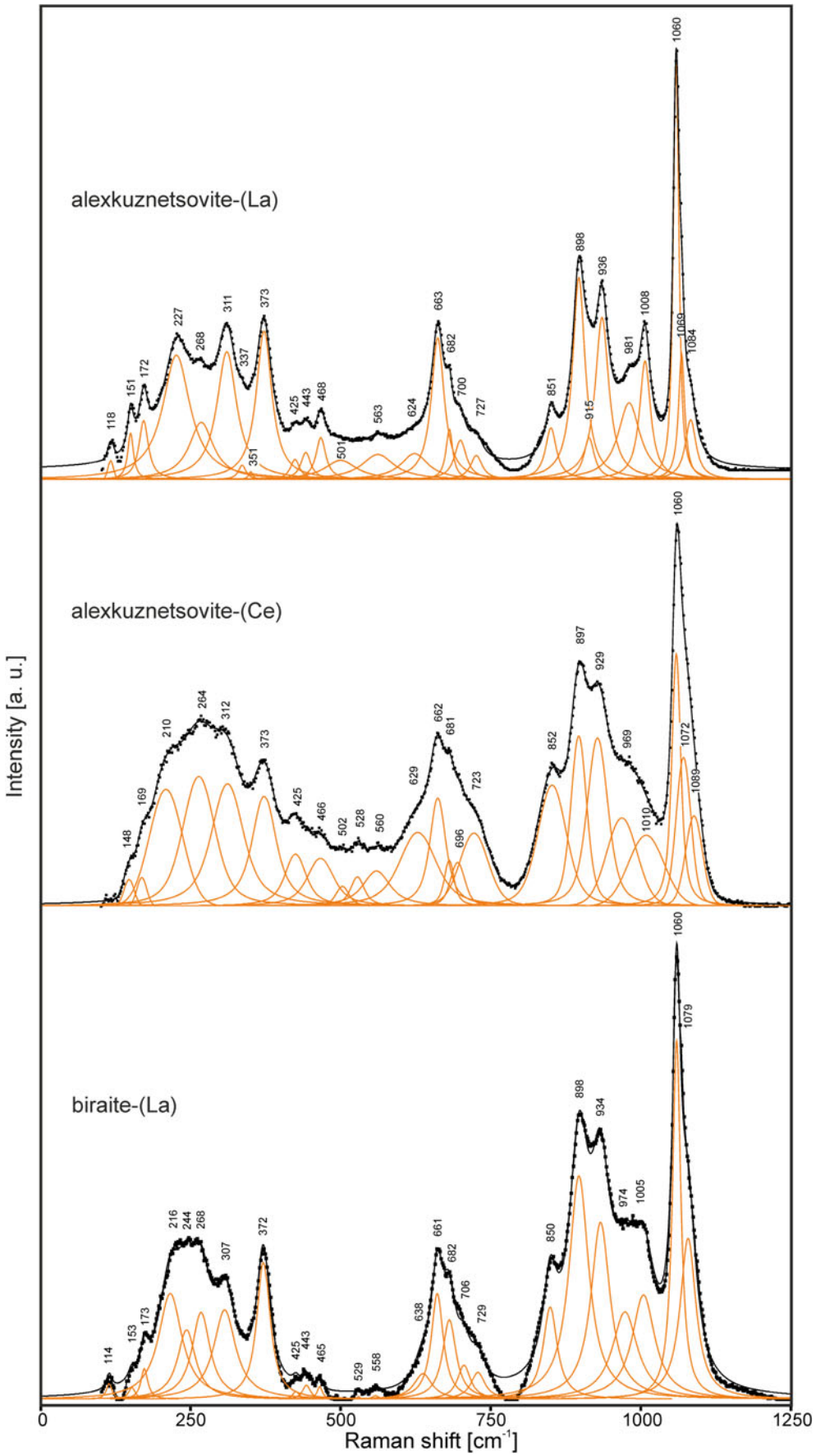

Fig. 4. Raman spectra of alexkuznetsovite-(La), alexkuznetsovite-(Ce) and biraite-(La) excited by 532 nm laser in the 100–1250 cm^{-1} region. The measured spectra are shown by dots. The curves matching to dots are a result of spectral fit as a sum of individual Voigt peaks shown below the curves.

https://doi.org/10.1180/mgm.2021.64 Published online by Cambridge University Press

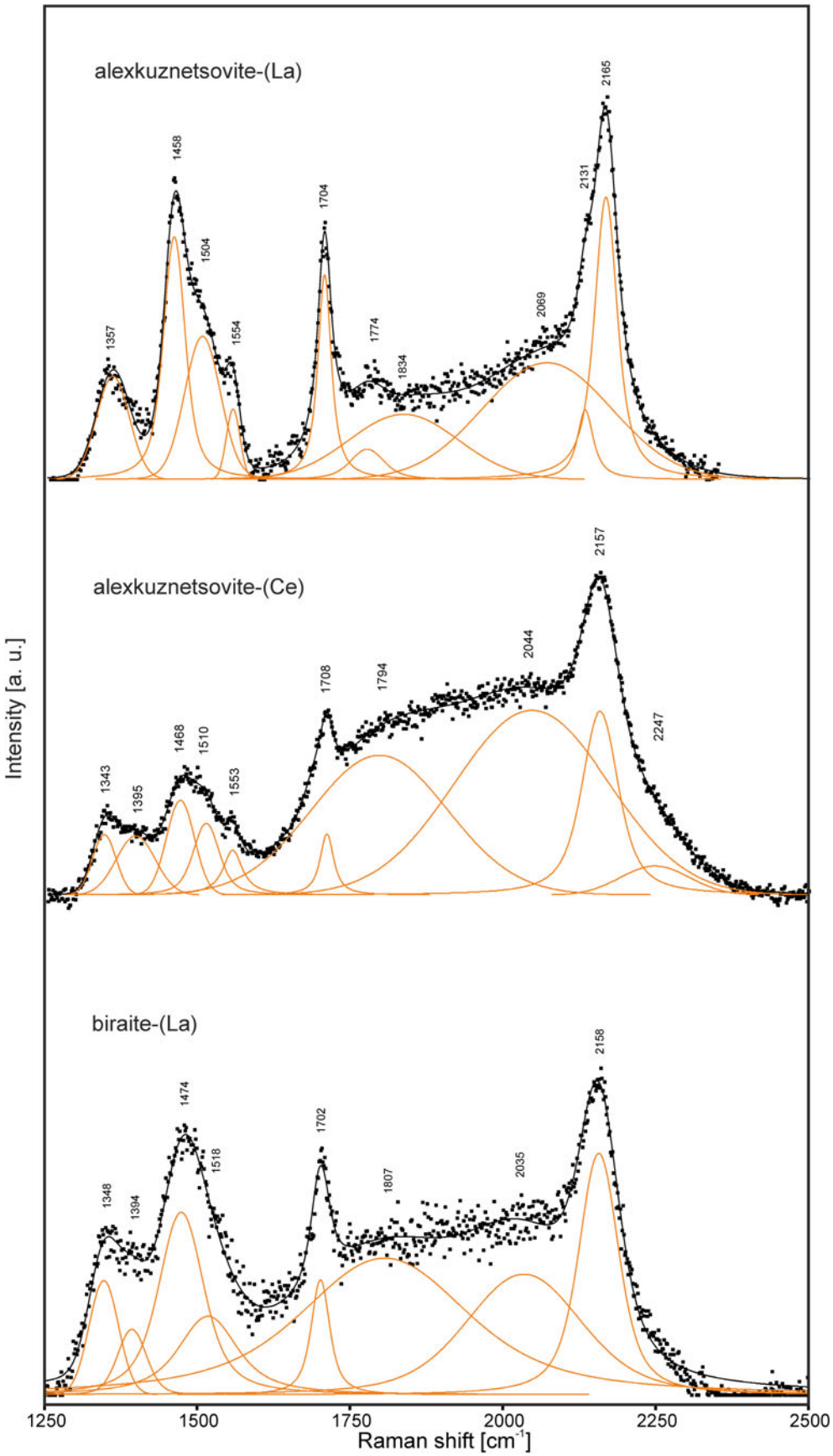

Fig. 5. Raman spectra of alexkuznetsovite-(La), alexkuznetsovite-(Ce) and biraite-(La) excited by 532 nm laser in 1250–2500 cm^{-1} region. The measured spectra are shown by dots. The curves matching to dots are a result of spectral fit as a sum of individual Voigt peaks shown below the curves.

https://doi.org/10.1180/mgm.2021.64 Published online by Cambridge University Press

Table 1. Average composition of alexkuznetsovite-(La), alexkuznetsovite-(Ce) and biraite-(La) (wt.%).

	Alexkuznetsovite-(La)			Alexkuznetsovite-(Ce)			Biraite-(La)			
Constituent	Mean, $n = 9$	Range	S.D.	Mean, $n = 8$	Range	S.D.	Mean, $n = 5$	Range	S.D.	Probe standard
CaO	1.20	1.16–1.33	0.07	1.42	1.25–1.66	0.20	1.24	1.12–1.47	0.16	wollastonite
La_2O_3	28.58	26.62–29.61	0.87	22.59	19.69–24.51	1.98	27.81	27.12–28.35	0.51	$LaPO_4$
Ce_2O_3	25.93	25.37–26.63	0.48	28.18	27.30–29.54	0.84	25.88	25.49–26.28	0.39	$CePO_4$
Pr_2O_3	1.37	1.24–1.45	0.09	2.17	1.83–2.61	0.34	1.29	1.20–1.41	0.09	$PrPO_4$
Nd_2O_3	2.89	2.58–3.26	0.27	4.91	4.48–5.23	0.27	2.56	2.13–3.03	0.41	$NdPO_4$
ThO_2	0.22	0.16–0.36	0.06	0.28	0.19–0.46	0.11	0.45	0.35–0.62	0.12	$CaTh(PO_4)_2$
MgO	0.25	0.19–0.44	0.08	0.17	0.11–0.44	0.15	0.48	0.42–0.52	0.04	Mg_2SiO_4
MnO*	6.34	5.21–7.29	0.64	6.35	4.70–8.01	1.50	4.82	4.71–4.95	0.10	spessartine
FeO*	3.66	3.36–4.17	0.31	4.22	3.01–5.97	1.09	5.67	5.43–5.81	0.17	almandine
SiO_2	21.46	21.01–21.76	0.21	21.45	21.33–21.76	0.18	21.67	21.51–21.78	0.14	sanidine
CO_2**	7.86			7.88			7.98			
H_2O**	0.10			0.11			0.19			
Total	99.86			99.73			100.04			

S.D. = standard deviation
* All iron and manganese are considered to be bivalent on the basis of structural data.
** Calculated by stoichiometry; the CO_3:HCO_3 ratio is calculated from the charge-balance requirement.

Table 2. Crystal data, data collection information and structure refinement details for alexkuznetsovite-(La), alexkuznetsovite-(Ce) and biraite-(La).

Mineral	Alexkuznetsovite-(La)	Alexkuznetsovite-(Ce)	Biraite-(La)
Crystal data			
Formula	$(LREE_{1.96}\square_{0.04})(Mn_{0.50}Fe_{0.29}Ca_{0.15}$ $LREE_{0.06})(H_{0.06}CO_3)(Si_2O_7)$*	$(LREE_{1.90}Ca_{0.06}Th_{0.01}\square_{0.03})$ $(Mn_{0.50}Fe_{0.33}Ca_{0.08}$ $LREE_{0.07}Mg_{0.02})(H_{0.07}CO_3)(Si_2O_7)$*	$(LREE_{1.88}Ca_{0.07}Th_{0.01}\square_{0.05})$ $(Fe_{0.44}Mn_{0.38}Mg_{0.07}$ $LREE_{0.06}Ca_{0.05})(H_{0.12}CO_3)(Si_2O_7)$*
Formula weight	564.10	558.02	554.20
Radiation and wavelength (Å)	Mo$K\alpha$; 0.71073	Mo$K\alpha$; 0.71073	Mo$K\alpha$; 0.71073
Crystal system, space group, Z	Monoclinic, $P2_1/c$, 4	Monoclinic, $P2_1/c$, 4	Monoclinic, $P2_1/c$, 4
Unit cell dimensions (Å/°)	$a = 6.5642(3)$, $b = 6.7689(3)$, $\beta = 108.684(6)$, $c = 18.7213(10)$	$a = 6.5764(4)$, $b = 6.7685(4)$, $\beta = 108.672(8)$, $c = 18.7493(15)$	$a = 6.5660(10)$, $b = 6.7666(11)$, $\beta = 108.952(16)$, $c = 18.698(3)$
V (Å^3)	788.00(7)	790.66(10)	785.7(2)
μ (mm^{-1})	12.76	13.12	12.46
F_{000}	1018	1012	1002
Crystal size (mm)	0.02 × 0.08 × 0.10	0.25 × 0.27 × 0.53	0.02 × 0.07 × 0.13
Data collection			
Diffractometer	Xcalibur S CCD	Xcalibur S CCD	Xcalibur S CCD
Temperature (K)	293(2)	293(2)	293(2)
Absorption correction	Gaussian	Gaussian	Gaussian
θ range (°)	3.221–28.274	3.221–28.266	3.223–28.271
Reflections collected	12664	13692	6283
Unique reflections	1947 ($R_{int} = 0.0658$)	1951 ($R_{int} = 0.0645$)	1941 ($R_{int} = 0.1374$)
Unique reflections [$I > 2\sigma(I)$]	1788	1844	1153
Refinement			
Structure solution/Refinement method	direct methods/full-matrix least-squares on F^2	full-matrix least-squares on F^2	full-matrix least-squares on F^2
Number of refined parameters	147	147	137
Final R indices [$I > 2\sigma(I)$]	$R_1 = 0.0628$, wR_2** = 0.1097	$R^1 = 0.0589$, wR_2** = 0.1181	$R_1 = 0.1194$, wR_2** = 0.1884
R indices (all data)	$R_1 = 0.0706$, wR_2** = 0.1122	$R_1 = 0.0634$, wR_2** = 0.1197	$R_1 = 0.1940$, wR_2** = 0.2212
GoF	1.336	1.325	1.120
Largest diff. peak / hole (e^-/Å^3)	2.22 [0.84 Å from *REE*2] and −1.57 [1.12 Å from O6]	2.63 [0.82 Å from *REE*1] and −1.74 [1.13 Å from O6]	3.00 [1.04 Å from *REE*1] and −1.59 [0.99 Å from *REE*1]

*Minor H^+ was added for charge balance assuming that O^{2-} at the O1 site is bonded with H^+ to form a HCO_3 group (see 'X-ray crystallography and crystal structure determination' section).
**$w = 1/[\sigma^2(F_o^2) + (0.0313P)^2 + 15.0469P]$; $P = \{[\max \text{ of } (0 \text{ or } F_o^2)] + 2F_c^2\}/3$ for alexkuznetsovite-(La)
$w = 1/[\sigma^2(F_o^2) + (0.0311P)^2 + 20.6291P]$; $P = \{[\max \text{ of } (0 \text{ or } F_o^2)] + 2F_c^2\}/3$ for alexkuznetsovite-(Ce)
$w = 1/[\sigma^2(F_o^2) + (0.0585P)^2 + 14.0043P]$; $P = \{[\max \text{ of } (0 \text{ or } F_o^2)] + 2F_c^2\}/3$ for biraite-(La)

O–C–O bending vibrations (doubly degenerate ν_4 mode) observed in the range of 700–730 cm^{-1} and split into a doublet because of the above-mentioned distortion of the CO_3 triangle.

The strongest band at 1060 cm^{-1} corresponds to symmetric C–O stretching vibrations of CO_3^{2-} anions (the nondegenerate ν_1 mode). The shoulders on the high-frequency slope of this band may correspond to Si–O stretching vibrations of the fragment Si–O–Si or symmetric C–O stretching in a different local environment (e.g. Ca instead of Mn or Fe).

The range 890 to 1010 cm^{-1} corresponds to stretching vibrations of apical Si–O bonds. The bands at 850–852 cm^{-1} are assigned to out-of-plane O–C–O bending vibrations (the nondegenerate ν_2 mode). The ranges 530 to 730 cm^{-1} and 400 to 510 cm^{-1} correspond to O–Si–O bending vibrations and combined Si–O–Si

https://doi.org/10.1180/mgm.2021.64 Published online by Cambridge University Press

Table 3. Atomic coordinates, equivalent displacement parameters (U_{eq}, in Å^2), site occupancy factors (s.o.f.) and bond-valence sums (BVS) for alexkuznetsovite-(La) (first line of each row), alexkuznetsovite-(Ce) (second line of each row) and biraite-(La) (third line of each row).

Site	*x*	*y*	*z*	U_{eq}	s.o.f.*	BVS
*REE*1	0.32551(11)	0.28158(10)	0.23652(4)	0.0151(2)	$La_{1.002(7)}$	3.21
	0.32530(11)	0.28033(10)	0.23671(4)	0.0196(2)	$Ce_{0.971(7)}$	2.95
	0.3272(3)	0.2740(3)	0.23759(10)	0.0265(6)	$La_{0.953(11)}$	3.24
*REE*2	0.88906(11)	0.86701(11)	0.07739(4)	0.0182(2)	$La_{0.998(6)}$	2.91
	0.88893(11)	0.86701(12)	0.07764(4)	0.0229(2)	$Ce_{0.969(7)}$	2.63
	0.8857(3)	0.8676(3)	0.07782(9)	0.0333(7)	$La_{0.981(11)}$	2.83
M	0.4295(3)	0.5112(3)	0.07754(10)	0.0290(6)	$Mn_{0.50}Fe_{0.29}Ca_{0.15}Ce_{0.06}$**	2.01
	0.4288(3)	0.5112(4)	0.07756(10)	0.0349(6)	$Mn_{0.50}Fe_{0.33}Ca_{0.08}Ce_{0.07}Mg_{0.02}$**	1.91
	0.4312(7)	0.5073(9)	0.0767(3)	0.0555(19)	$Fe_{0.44}Mn_{0.38}Mg_{0.07}LREE_{0.06}Ca_{0.05}$**	1.99
Si1	0.9228(5)	0.3566(5)	0.07364(18)	0.0149(7)	$Si_{1.00}$	3.95
	0.9232(5)	0.3557(5)	0.07410(18)	0.0190(7)		3.93
	0.9244(13)	0.3528(14)	0.0739(4)	0.032(2)		3.92
Si2	0.8041(5)	0.2865(5)	0.21853(17)	0.0128(7)	$Si_{1.00}$	3.94
	0.8046(5)	0.2847(5)	0.21862(17)	0.0169(7)		3.97
	0.8061(11)	0.2793(12)	0.2186(4)	0.0232(18)		4.01
C	0.4019(18)	0.9874(18)	0.0984(7)	0.017(2)	$C_{1.00}$	3.77
	0.399(2)	0.9856(19)	0.0973(7)	0.027(3)		3.73
	0.390(3)	0.976(3)	0.0933(12)	0.027(6)***		3.73
O1	0.4174(14)	0.1315(14)	0.0556(5)	0.027(2)	$O_{1.00}$	1.74
	0.4176(15)	0.1314(15)	0.0557(5)	0.032(2)		1.70
	0.420(3)	0.126(3)	0.0552(10)	0.046(6)		1.73
O2	0.2681(13)	−0.0086(13)	0.1366(5)	0.0207(19)	$O_{1.00}$	1.98
	0.2680(13)	−0.0086(14)	0.1371(5)	0.0260(19)		1.90
	0.271(3)	−0.013(3)	0.1379(10)	0.040(6)		1.92
O3	0.5367(14)	0.8345(13)	0.1092(5)	0.025(2)	$O_{1.00}$	1.99
	0.5370(15)	0.8341(15)	0.1099(5)	0.032(2)		1.93
	0.529(3)	0.826(3)	0.1083(12)	0.047(6)		1.99
O4	0.9111(13)	0.1892(13)	0.0116(5)	0.0214(19)	$O_{1.00}$	1.93
	0.9107(14)	0.1906(14)	0.0113(5)	0.0265(19)		1.83
	0.910(3)	0.192(3)	0.0098(9)	0.034(5)		1.91
O5	0.1488(14)	0.4669(14)	0.1079(5)	0.025(2)	$O_{1.00}$	1.85
	0.1514(15)	0.4652(16)	0.1096(5)	0.034(2)		1.82
	0.156(3)	0.457(3)	0.1090(11)	0.046(6)		1.82
O6	0.7303(14)	0.5174(13)	0.0433(5)	0.0225(19)	$O_{1.00}$	2.01
	0.7313(14)	0.5178(14)	0.0441(5)	0.0266(19)		1.94
	0.727(3)	0.509(3)	0.0437(11)	0.039(5)***		1.99
O7	0.8900(13)	0.2250(12)	0.1456(4)	0.0164(17)	$O_{1.00}$	2.07
	0.8897(13)	0.2249(13)	0.1455(4)	0.0211(17)		2.07
	0.890(3)	0.215(3)	0.1451(9)	0.025(4)		2.07
O8	0.6598(13)	0.1168(12)	0.2369(5)	0.0183(18)	$O_{1.00}$	2.21
	0.6600(13)	0.1163(13)	0.2372(5)	0.0252(19)		2.08
	0.670(2)	0.109(2)	0.2389(9)	0.031(5)		2.23
O9	0.0230(13)	0.3262(14)	0.2867(5)	0.021(2)	$O_{1.00}$	1.97
	0.0233(13)	0.3224(14)	0.2861(5)	0.0246(19)		1.89
	0.027(3)	0.314(3)	0.2870(10)	0.030(5)		2.01
O10	0.6374(13)	0.4713(12)	0.1927(5)	0.0182(18)	$O_{1.00}$	2.04
	0.6380(13)	0.4696(13)	0.1936(5)	0.0235(18)		1.96
	0.638(3)	0.462(3)	0.1942(11)	0.038(5)		2.05

Notes: Parameters were taken from Gagné and Hawthorne (2015). For BVS the values were calculated taking into account the assigned occupancy of the *M* site. Parameters of La were used for both *REE* sites for alexkuznetsovite-(La) and biraite-(La) and parameters of Ce were used for both *REE* sites for alexkuznetsovite-(Ce). The low BVS value for O(1) is typical also for isostructural biraite-(Ce) (Konev *et al.*, 2005) and is possibly connected with steric restrictions for interatomic distances.
*The La scattering curve was used during the structure refinement for *REE* in alexkuznetsovite-(La) and biraite-(La) and Ce scattering curve was used for alexkuznetsovite-(Ce).
**Fixed during the refinement.
***U_{iso}

bending and *M*–O stretching vibrations, respectively. Bands below 380 cm^{-1} are due to lattice vibrations involving relative shifts of *REE* cations, $Si_2O_7^{6-}$ and CO_3^{2-} groups as a whole.

The bands at 1702–1708 cm^{-1} correspond to the first overtone of the band of out-of-plane O–C–O bending vibrations at 850–852 cm^{-1}. The bands observed in the range of 2157–2165 cm^{-1} may correspond to a combination mode (a combination of stretching and bending vibrations of CO_3^{2-} anions). Relatively high intensities of these bands reflect a high anharmonicity of corresponding vibrations which may be due to the distortion of the CO_3^{2-} group.

Taking into account high widths of the weak bands in the range of 1770–2070 cm^{-1}, they cannot be assigned to any combination modes or overtones. These absorptions may be due to luminescence. On the contrary, vibrational (Raman and infrared) spectra of acid carbonates contain broad and weak bands whose positions vary in the wide range from 1690 to 2600 cm^{-1} (Kagi *et al.*, 2003; Jentzsch *et al.*, 2013; Chukanov, 2014; Chukanov and Chervonnyi, 2016). Consequently, the presence of minor amounts of HCO_3^- groups in the samples studied cannot be excluded. This assumption is in agreement with compositional and structural data (see below).

No distinct bands are observed above 3000 cm^{-1}.

https://doi.org/10.1180/mgm.2021.64 Published online by Cambridge University Press

Chemical composition

Chemical data for the new minerals were obtained using a Cameca SX-100 electron microprobe (wavelength-dispersive spectroscopy mode, acceleration voltage of 15 kV, a beam current of 20 nA and a 5 μm beam diameter). CO_2 was not determined directly due to the scarcity of pure material but calculated from stoichiometry. H_2O content was calculated on the basis of the charge-balance requirement and by taking into account the Raman spectra which indicate the presence of minor amounts of HCO_3^- groups. All iron and manganese were considered to be bivalent on the basis of structural data.

Analytical data are given in Table 1. Contents of other elements with atomic numbers higher than that of carbon are below detection limits.

The chemical composition of the minerals studied is slightly variable, particularly in the *REE* proportions and the Fe and Mn content. The Ca and Mg contents varies from 0.10–0.16 and 0.02–0.08 atoms per formula unit (apfu), respectively. Taking into account structural data (see below), the charge-balanced empirical formulae of holotype specimens calculated on the basis of 2 Si and 10 O apfu are: alexkuznetsovite-(La), $(La_{0.98}Ce_{0.89}Nd_{0.10}Pr_{0.05})_{\Sigma 2.02}(Mn^{2+}_{0.50}Fe^{2+}_{0.29}Ca_{0.12}Mg_{0.03})_{\Sigma 0.94}(CO_3)_{0.94}(HCO_3)_{0.06}(Si_2O_7)$; alexkuznetsovite-(Ce), $(Ce_{0.96}La_{0.78}Nd_{0.16}Pr_{0.07}Th_{0.01})_{\Sigma 1.98}(Mn^{2+}_{0.50}Fe^{2+}_{0.33}Ca_{0.14}Mg_{0.02})_{\Sigma 0.99}(CO_3)_{0.93}(HCO_3)_{0.07}(Si_2O_7)$; and biraite-(La) $(La_{0.95}Ce_{0.87}Nd_{0.08}Pr_{0.04}Th_{0.01})_{\Sigma 1.95}(Fe^{2+}_{0.44}Mn^{2+}_{0.38}Ca_{0.12}Mg_{0.07})_{\Sigma 1.01}(CO_3)_{0.88}(HCO_3)_{0.12}(Si_2O_7)$.

The idealised formulae are as follows. Alexkuznetsovite-(La): $La_2Mn(CO_3)(Si_2O_7)$, which requires MnO 12.64, La_2O_3 58.08, CO_2 7.85, SiO_2 21.43, total 100 wt.%. Alexkuznetsovite-(Ce): $Ce_2Mn(CO_3)(Si_2O_7)$, which requires MnO 12.60, Ce_2O_3 58.26, CO_2 7.81, SiO_2 21.33, total 100 wt.%. Biraite-(La): $La_2Fe^{2+}(CO_3)(Si_2O_7)$, which requires FeO 12.78, La_2O_3 58.01, CO_2 7.83, SiO_2 21.38, total 100 wt.%.

X-ray crystallography and crystal structure determination

Powder XRD data for all three minerals (Supplementary tables S1–S3) were collected with a Rigaku R-AXIS Rapid II single-crystal diffractometer equipped with a cylindrical image plate detector (radius 127.4 mm) using Debye-Scherrer geometry, Co*K*α radiation (rotating anode with VariMAX microfocus optics), 40 kV, 15 mA and exposure of 15 min. Angular resolution of the detector is 0.045°2θ (pixel size is 0.1 mm). The data were integrated using the software package *Osc2Tab* (Britvin *et al.*, 2017). Parameters of monoclinic unit cells refined from the powder XRD data are for alexkuznetsovite-(La): $a = 6.565(8)$, $b = 6.807(5)$, $c = 18.78(2)$ Å, $\beta = 108.52(9)°$ and $V = 796(2)$ Å^3; for alexkuznetsovite-(Ce): $a = 6.576(6)$, $b = 6.720(3)$, $c = 18.78(2)$ Å, $\beta = 108.73(7)°$ and $V = 786(1)$ Å^3; and for biraite-(La): $a = 6.574(5)$, $b = 6.772(3)$, $c = 18.79(2)$ Å, $\beta = 108.81(8)°$ and $V = 792(2)$ Å^3. The difference between the unit-cell parameters determined using powder XRD and those obtained by single-crystal XRD studies may be derived from the chemical heterogeneity of measured grains.

Single-crystal XRD studies of all new minerals were carried out using an Xcalibur S diffractometer equipped with a CCD detector for grains analysed by electron microprobe and then extracted from the polished sections. A full sphere of three-dimensional data was collected. Data reduction was performed using *CrysAlisPro* Version 1.171.37.35 (Rigaku, 2018). The data were corrected for Lorentz factor and polarisation effects.

Table 4. Selected interatomic distances (Å) in the structures of alexkuznetsovite-(La), alexkuznetsovite-(Ce) and biraite-(La).

Alexkuznetsovite-(La)		Alexkuznetsovite-(Ce)		Biraite-(La)	
*REE*1–O8	2.318(9)	*REE*1–O8	2.322(9)	*REE*1–O8	2.311(14)
*REE*1–O10	2.453(8)	*REE*1–O10	2.447(9)	*REE*1–O10	2.44(2)
*REE*1–O8'	2.459(8)	*REE*1–O9	2.461(8)	*REE*1–O9	2.447(17)
*REE*1–O9	2.473(8)	*REE*1–O8'	2.462(8)	*REE*1–O8'	2.503(17)
*REE*1–O5	2.631(9)	*REE*1–O5	2.610(10)	*REE*1–O5	2.61(2)
*REE*1–O2	2.654(8)	*REE*1–O2	2.647(9)	*REE*1–O2	2.634(19)
*REE*1–O10'	2.754(8)	*REE*1–O3	2.748(9)	*REE*1–O10'	2.742(18)
*REE*1–O3	2.759(9)	*REE*1–O10'	2.755(8)	*REE*1–O3	2.75(2)
*REE*1–O7	2.845(8)	*REE*1–O7	2.852(8)	*REE*1–O7	2.857(17)
REE1–O2'	*3.273(9)*	*REE1–O2'*	*3.278(9)*	*REE1–O2'*	*3.23(2)*
<*REE*1–O>	2.662	<*REE*1–O>	2.658	<*REE*1–O>	2.652
*REE*2–O9	2.437(8)	*REE*2–O9	2.452(8)	*REE*2–O9	2.430(17)
*REE*2–O4	2.459(8)	*REE*2–O4	2.464(8)	*REE*2–O4	2.466(17)
*REE*2–O2	2.522(8)	*REE*2–O2	2.527(8)	*REE*2–O2	2.545(18)
*REE*2–O4'	2.531(9)	*REE*2–O4'	2.546(9)	*REE*2–O4'	2.569(19)
*REE*2–O3	2.576(9)	*REE*2–O6	2.577(10)	*REE*2–O3	2.600(18)
*REE*2–O6	2.582(9)	*REE*2–O3	2.583(9)	*REE*2–O6	2.64(2)
*REE*2–O1	2.652(9)	*REE*2–O1	2.661(9)	*REE*2–O1	2.641(18)
*REE*2–O7	2.739(8)	*REE*2–O7	2.736(8)	*REE*2–O7	2.661(17)
REE2–O5	*3.154(10)*	*REE2–O5*	*3.174(11)*	*REE2–O5*	*3.24(2)*
<*REE*2–O>	2.628	<*REE*2–O>	2.636	<*REE*2–O>	2.644
M–O5	2.117(9)	*M*–O5	2.118(9)	*M*–O5	2.112(19)
M–O10	2.168(9)	*M*–O10	2.188(9)	*M*–O6	2.154(19)
M–O6	2.176(8)	*M*–O6	2.194(9)	*M*–O10	2.20(2)
M–O6'	2.264(8)	*M*–O6'	2.270(9)	*M*–O6'	2.220(18)
M–O3	2.317(9)	*M*–O3	2.319(10)	*M*–O3	2.28(2)
M–O1	2.600(10)	*M*–O1	2.600(11)	*M*–O1	2.61(2)
M–O4	*3.083(9)*	*M–O4*	*3.074(10)*	*M–O4*	*3.07(2)*
<*M*–O>	2.389	<*M*–O>	2.395	<*M*–O>	2.378
Si1–O5	1.600(9)	Si1–O4	1.606(9)	Si1–O4	1.597(18)
Si1–O4	1.606(9)	Si1–O5	1.614(9)	Si1–O5	1.61(2)
Si1–O6	1.626(9)	Si1–O6	1.630(9)	Si1–O6	1.63(2)
Si1–O7	1.686(8)	Si1–O7	1.678(8)	Si1–O7	1.700(17)
<Si–O>	1.630	<Si–O>	1.632	<Si–O>	1.634
Si2–O8	1.596(9)	Si2–O8	1.593(9)	Si2–O8	1.576(9)
Si2–O9	1.610(8)	Si2–O9	1.603(9)	Si2–O9	1.610(18)
Si2–O10	1.630(8)	Si2–O10	1.630(9)	Si2–O10	1.62(2)
Si2–O7	1.687(8)	Si2–O7	1.687(8)	Si2–O7	1.696(17)
<Si2–O>	1.631	<Si2–O>	1.628	<Si2–O>	1.626
C–O1	1.288(14)	C–O1	1.288(15)	C–O1	1.291(10)
C–O2	1.299(13)	C–O2	1.310(13)	C–O2	1.315(10)
C–O3	1.334(14)	C–O3	1.338(14)	C–O3	1.327(10)
<C–O>	1.307	<C–O>	1.312	<C–O>	1.311

Elongated *REE*–O distances and strongly elongated *M*–O4 bonds not included in the *M*-centred octahedra are given in italic.

The crystal structure of alexkuznetsovite-(La) was solved by direct methods and refined using the *SHELX* software package (Sheldrick, 2015) to $R = 0.0628$ for 1788 unique reflections with $I > 2\sigma(I)$. The crystal structure of alexkuznetsovite-(Ce) was obtained using a model of alexkuznetsovite-(La) as the starting one and refined using *SHELX* to $R = 0.0589$ for 1844 unique reflections with $I > 2\sigma(I)$. The crystal structure of biraite-(La) was refined using *SHELX* to $R = 0.1194$ for 1153 unique reflections with $I > 2\sigma(I)$ and with the model of alexkuznetsovite-(La) as an initial one. Unfortunately, even the best single crystal of biraite-(La) showed a low quality that caused a rather large final *R* value: 11.93%. This might be due to the two times higher ThO_2 content relative to alexkuznetsovite-(La) that could cause stronger radiation-induced structural damage. We consider our results as a structural model only.

https://doi.org/10.1180/mgm.2021.64 Published online by Cambridge University Press

Table 5. Refined site-scattering factors and assignment for *REE* and *M* cation sites in the structure of alexkuznetsovite-(La), alexkuznetsovite-(Ce) and biraite-(La).*

Site	SC	s.o.f.	SSF_{exp} (e^-)	Assigned occupancy	SSF_{calc} (e^-)
Alexkuznetsovite-(La)					
*REE*1	La	1.002	57.11	$La_{0.49}Ce_{0.415}Nd_{0.05}Pr_{0.025}\square_{0.02}$	56.48
*REE*2	La	0.998	56.89	$La_{0.49}Ce_{0.415}Nd_{0.05}Pr_{0.025}\square_{0.02}$	56.48
M	Mn	1.07	26.75	$Mn_{0.50}Fe_{0.29}Ca_{0.15}Ce_{0.06}$	26.52
Alexkuznetsovite-(Ce)					
*REE*1	Ce	0.971	56.32	$Ce_{0.445}La_{0.39}Nd_{0.08}Pr_{0.035}Ca_{0.03}Th_{0.005}\square_{0.015}$	55.96
*REE*2	Ce	0.969	56.20	$Ce_{0.445}La_{0.39}Nd_{0.08}Pr_{0.035}Ca_{0.03}Th_{0.005}\square_{0.015}$	55.96
M	Mn	1.10	27.50	$Mn_{0.50}Fe_{0.33}Ca_{0.08}Ce_{0.07}Mg_{0.02}$	26.98
Biraite-(La)					
*REE*1	La	0.953	54.32	$La_{0.475}Ce_{0.405}Nd_{0.040}Pr_{0.020}Ca_{0.02}\square_{0.04}$	54.54
*REE*2	La	0.981	55.92	$La_{0.475}Ce_{0.405}Nd_{0.040}Pr_{0.020}Ca_{0.05}Th_{0.01}$	56.05
M	Fe	1.01	26.26	$Fe_{0.44}Mn_{0.38}Mg_{0.07}LREE_{0.06}Ca_{0.05}$	26.26

*SC is the scattering curve used for the refinement of site occupancy; s.o.f is the refined site occupancy factor; SSF_{exp} and SSF_{calc} are the experimental and calculated site-scattering factors, respectively. Minor discrepancies between SSFexp (e^-) and SSFcalc (e^-) are within the limits of analytical errors and chemical inhomogeneity of the mineral. The main 'artificial' cause of these discrepancies could be due to using of scattering curve of La, the lightest of *LREE* for alexkuznetsovite-(La) and biraite-(La), and Ce for alexkuznetsovite-(Ce) during the structure refinement.

The crystal data, data collection information and structure refinement details for all the new minerals are summarised in Table 2, atomic coordinates, thermal displacement parameters of atoms, site occupancies and bond-valence sums are given in Table 3 and selected interatomic distances in Table 4. Refined site-scattering factors and the assignment for *REE* and *M* cation sites in the structure of all three minerals are given in Table 5. The crystallographic information files for the new minerals have been deposited with the Principal Editor of *Mineralogical Magazine* and are available as Supplementary material (see below).

Crystal chemistry and genesis of biraite-group minerals from Mochalin Log: results and discussion

Alexkuznetsovite-(La), alexkuznetsovite-(Ce) and biraite-(La) are isostructural (Figs 6 and 7). Their structures (Figs 6a, b) are based on (001) heteropolyhedral layers built by dimers of edge-sharing *M*-centred polyhedra connected *via* disilicate groups [Si_2O_7] and CO_3 triangles (Fig. 7). The Si(1)–O(7)–Si(2) angles in the disilicate groups of all three species are rather small and very close to each other: 132.7(5)° in alexkuznetsovite-(La), 133.2(6)° in alexkuznetsovite-(Ce) and 130.8(11)° in biraite-(La). The [Si_2O_7] groups are fixed at the O(6)–O(10) edges of the *M*-centred octahedra. $LREE^{3+}$ cations provide linkages between adjacent layers.

There are two crystallographically non-equivalent *LREE* sites located in the large intra- and inter-layer sites. The *LREE*1 site occupies nine-fold polyhedra with distances in the ranges 2.318(9)–2.845(8), 2.322(9)–2.852(8) and 2.311(14)–2.857(17) Å with elongated *LREE*1–O2 distances of 3.273(9), 3.278(9) and 3.23(2) Å for alexkuznetsovite-(La), alexkuznetsovite-(Ce) and biraite-(La), respectively. *LREE*2 site occupies eight-fold polyhedra with the distances in the ranges 2.437(8)–2.739(8), 2.452(8)–2.736(8) and 2.430(17)–2.661(17) Å with elongated *LREE*2–O5 distances of 3.154(10), 3.174(11) and 3.24(2) Å for alexkuznetsovite-(La), alexkuznetsovite-(Ce) and biraite-(La), respectively. According to the refinement of site occupation factor (s.o.f.), both sites are occupied by $LREE^{3+}$ cations. According to chemical data La is a dominant component in alexkuznetsovite-(La) and biraite-(La), along

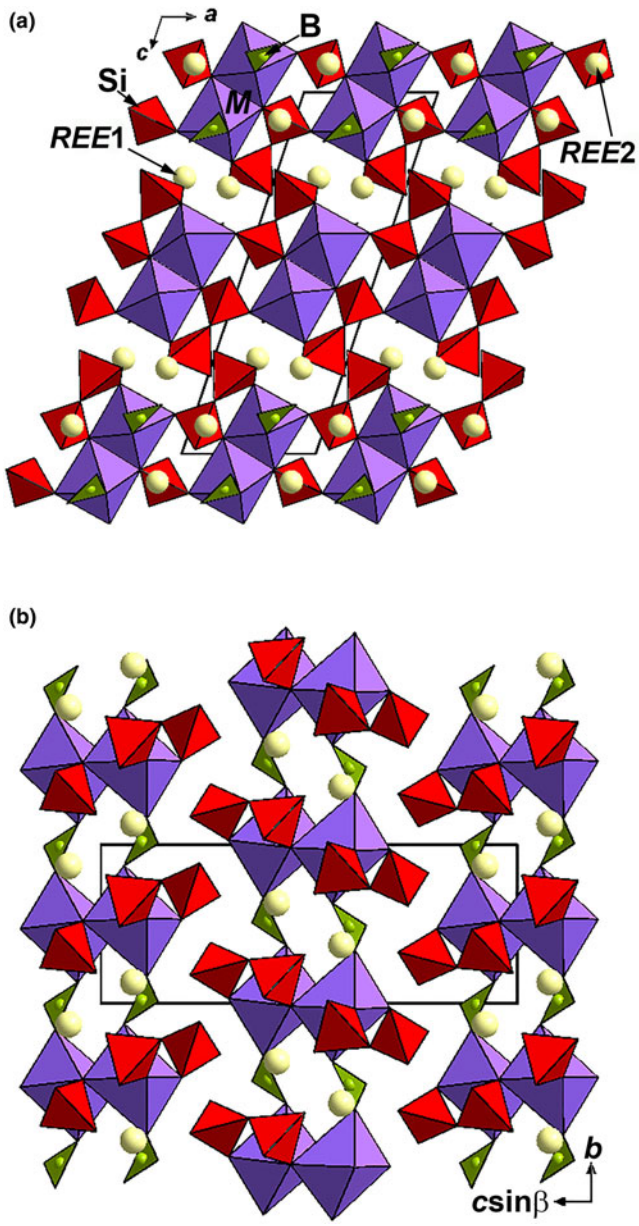

Fig. 6. The crystal structure of alexkuznetsovite-(La)/alexkuznetsovite-(Ce)/biraite-(La) projected along the *b* (a) and *c* (b) axes. The unit cell is outlined.

with subordinate Ce, minor Nd, Pr and vacancy (in biraite-(La) there is also very minor Ca and Th). In alexkuznetsovite-(Ce) Ce is a dominant component according to chemical data with subordinate La, minor Nd and Pr, and very minor Ca, Th and vacancy (Table 5). The presence of the very minor vacancy at the *LREE* sites was assumed on the basis of chemical analyses which always resulted in a small but reproducible general deficiency of all metal cations: instead of *ca.* 3.00 apfu (2*REE* +1 Mn/Fe), as should be expected from the ideal formula, this sum was within the 2.94–2.98 range in all analyses of alexkuznetsovite-(La), alexkuznetsovite-(Ce) and biraite-(La).

In alexkuznetsovite-(La) and alexkuznetsovite-(Ce) the *M* site is Mn^{2+}-dominant with subordinate Fe^{2+} and minor Ca, Mg and *LREE*. In biraite-(La) it is Fe^{2+}-dominant with subordinate Mn^{2+} and minor Mg, Ca and *LREE*. The location of a minor amount (~6–7%) of *LREE* in the relatively small *M*-centred octahedron

https://doi.org/10.1180/mgm.2021.64 Published online by Cambridge University Press

Table 6. Comparative data for minerals of the biraite group.

Mineral	Alexkuznetsovite-(La)	Alexkuznetsovite-(Ce)	Biraite-(La)	Biraite-(Ce)
End-member formula	$La_2Mn^{2+}(CO_3)(Si_2O_7)$	$Ce_2Mn^{2+}(CO_3)(Si_2O_7)$	$La_2Fe^{2+}(CO_3)(Si_2O_7)$	$Ce_2Fe^{2+}(CO_3)(Si_2O_7)$
Empirical formula	$(La_{0.98}Ce_{0.89}Nd_{0.10}Pr_{0.05})_{\Sigma 2.02}$ $Mn^{2+}_{0.50}Fe^{2+}_{0.29}Ca_{0.12}Mg_{0.03}$ $(CO_3)_{0.94}(HCO_3)_{0.06}(Si_2O_7)$	$(Ce_{0.96}La_{0.78}Nd_{0.16}Pr_{0.07})_{\Sigma 1.97}$ $Th_{0.01}Mn^{2+}_{0.50}Fe^{2+}_{0.33}Ca_{0.14}Mg_{0.02}$ $(CO_3)_{0.93}(HCO_3)_{0.07}(Si_2O_7)$	$(La_{0.95}Ce_{0.87}Nd_{0.08}Pr_{0.04})_{\Sigma 1.94}$ $Th_{0.01}Ca_{0.12}Fe^{2+}_{0.44}Mn^{2+}_{0.38}Mg_{0.07}$ $(CO_3)_{0.88}(HCO_3)_{0.12}(Si_2O_7)$	$(Ce_{1.01}La_{0.57}Nd_{0.25}Pr_{0.09}Sm_{0.02}$ $Ca_{0.07}Na_{0.02}Ba_{0.01})_{\Sigma 2.04}$ $(Fe_{0.60}Mg_{0.25}Mn_{0.11}Ti_{0.01})_{\Sigma 0.97}$ $(CO_3)_{0.99}$ $[Si_{1.97}(O_{6.87}F_{0.17})_{\Sigma 7.04}]$
Crystal system	Monoclinic	Monoclinic	Monoclinic	Monoclinic
Space group	$P2_1/c$	$P2_1/c$	$P2_1/c$	$P2_1/c$
a (Å)	6.5642(3)	6.5764(4)	6.5660(10)	6.505(7)
b (Å)	6.7689(3)	6.7685(4)	6.7666(11)	6.744(2)
c Å)	18.7213(10)	18.7493(15)	18.698(3)	18.561(4)
β (°)	108.684(6)	108.672(8)	108.952(16)	108.75(2)
V (Å^3)	788.00(7)	790.66(10)	785.7(2)	771.1(2)
Z	4	4	4	4
Strong reflections	4.595–63	4.145–35	4.594–49	3.30–50
of the powder	4.208–50	3.177–26	3.055–100	3.14–40
XRD pattern:	3.171–49	2.893–100	2.962–66	2.92–100
d, Å – *I*, %	2.962–100	2.797–36	2.787–35	2.65–50
	2.785–76	1.833–26	2.690–38	2.23–50
Colour	Brown to dark brown	Brown to dark brown	Brown to dark brown	Brown to light grey
Lustre	Vitreous	Vitreous	Vitreous	Vitreous
Density (calc.), (g cm^{-3})	4.713	4.687	4.682	4.76
Optical data:	Biaxial (–)	Biaxial (–)	Biaxial (–)	Biaxial (–)
α	1.780(6)	1.790(6)	1.770(5)	1.785(1)
β	1.807(6)	1.812(6)	1.790(5)	1.810(2)
γ	1.818(6)	1.824(8)	1.800(5)	1.820(1)
$2V_{meas.}$ (°)	65(10)	70(10)	70(10)	66(1)
Source	This paper	This paper	This paper	Konev *et al.* (2005)

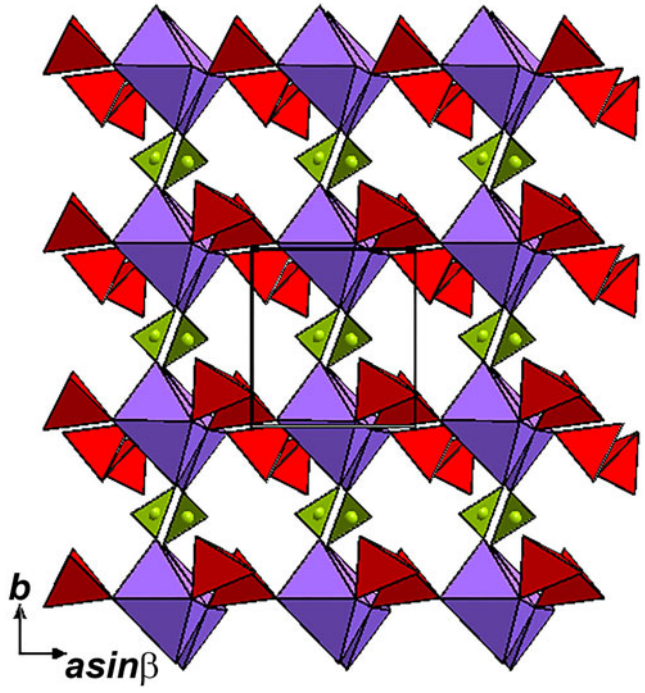

Fig. 7. Heteropolyhedral layer in the structure of alexkuznetsovite-(La)/alexkuznetsovite-(Ce)/biraite-(La). The unit cell is outlined. For legend see Fig. 6.

in the structure of alexkuznetsovite-(La)/alexkuznetsovite-(Ce)/biraite-(La) is caused by the refined number of electrons (e_{ref} = 26.75/27.50/26.26, respectively) and taking into account the longest *M*–O(1) distances of 2.600(10)/2.600(11)/2.61(2) Å in the *M*-centred octahedra and the existence of the bonds with the *M*–O(4) distance of 3.083(9)/3.074(10)/3.07(2) Å. These strongly elongated bonds are given in italics in Table 4. The average *M*–O distance is 2.389/2.395/2.37 Å. Thus, on the basis of electron-microprobe data and e_{ref}, both *REE* sites in alexkuznetsovite-(La) with almost equal s.o.f. (e_{ref} = 57.11 for the La1 site and 56.89 for La2) were assumed to be occupied by $LREE_{1.96}\square_{0.04}$ (□ = vacancy) and the *M* site by $Mn_{0.50}Fe_{0.29}Ca_{0.15}LREE_{0.06}$; in alexkuznetsovite-(Ce) (e_{ref} 56.32 for Ce1 and 56.20 for Ce2) – by $LREE_{1.90}Ca_{0.06}Th_{0.01}\square_{0.03}$ and $Mn_{0.50}Fe_{0.33}Ca_{0.08}LREE_{0.07}Mg_{0.02,}$ and in biraite-(La) (e_{ref} 54.32 for La1 and 55.92 for La2) – by $LREE_{1.88}Ca_{0.07}Th_{0.01}\square_{0.04}$ and $Fe_{0.44}Mn_{0.38}Mg_{0.07}LREE_{0.06}Ca_{0.05}$, respectively (Table 5). On the basis of the Raman spectra of the minerals and taking into account a significant distortion of the CO_3 triangle, we assume that insignificant lack of positive charge in their empirical formulae could be balanced by minor incorporation of H^+ (bonded with oxygen at the O1 site with formation of HCO_3 group: see above) which is characterised by relatively low bond-valence sums of 1.74, 1.70 and 1.73 for alexkuznetsovite-(La), alexkuznetsovite-(Ce) and biraite-(La), respectively (Table 3). It is worth noting that the lowering of bond-valence sum for the O1 site was previously reported also for biraite-(Ce) (Konev *et al.*, 2005). The presence of minor Ce^{4+} as a supposed compensator of the positive charge deficiency seems hardly probable due to distinctly reducing conditions of formation of the mineral assemblages with alexkuznetsovite-(La), alexkuznetsovite-(Ce), biraite-(La) and other *REE* silicates and carbonates, as well as associated minerals: they contain only Fe^{2+} and Mn^{2+}.

As noted above, all three new species from Mochalin Log are isostructural to each other and to biraite-(Ce), described earlier from the Biraya *REE*–Fe occurrence, Irkutsk Oblast, Siberia, Russia (Konev *et al.*, 2005). For comparison of all four members of the biraite group see Table 6. An elevated content of Mg (0.25 apfu) in biraite-(Ce) form Biraya suggests a hypothetical Mg-dominant member.

https://doi.org/10.1180/mgm.2021.64 Published online by Cambridge University Press

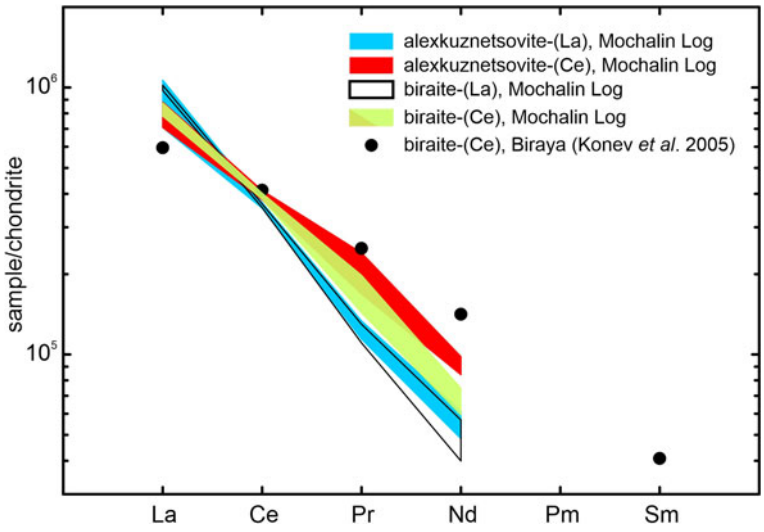

Fig. 8. Chondrite (McDonough and Sun, 1995) normalised *REE* pattern of biraite-group minerals from Mochalin Log and the original biraite-(Ce) from Biraya, Siberia, Russia (Konev *et al.*, 2005) for comparison.

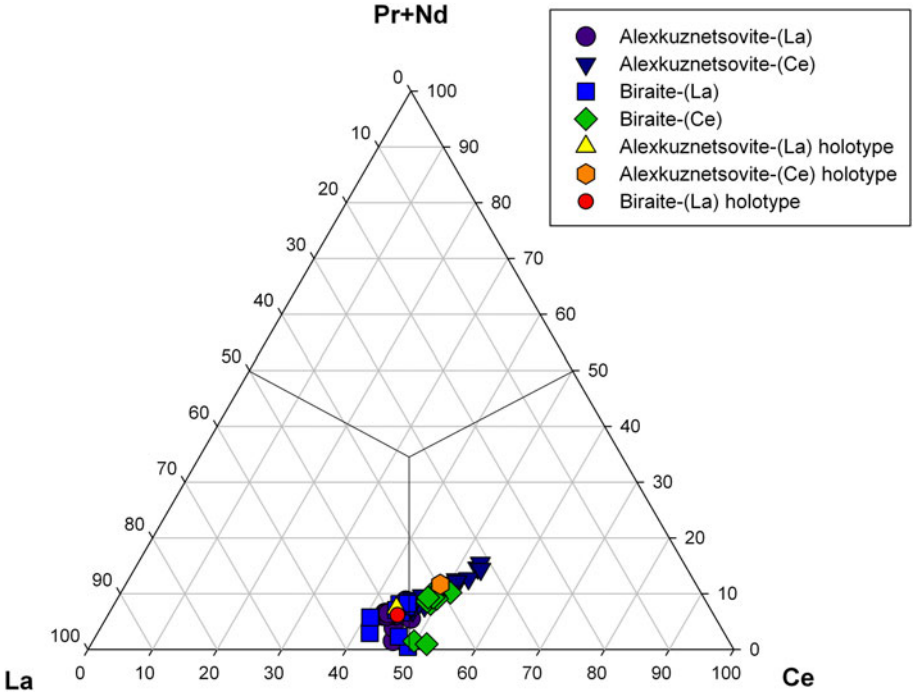

Fig. 9. Ternary plot showing distribution of *REE* at *A* sites in minerals of the biraite group.

Our electron microprobe analyses show two main schemes of isomorphic substitutions in the minerals of the biraite group: (1) La ↔ Ce at the *A* sites and (2) Mn^{2+} ↔ Fe^{2+} at the *M* site. The impoverishment of La is always accompanied by enrichment in other *LREE*, see Fig 8. In our previous papers we noted that a typical feature of Mochalin Log *REE* assemblage is its enrichment in *LREE*, especially La and Ce, coupled with a practically total absence of *HREE* and Y, and the wide variation of La and Ce contents in most of the samples studied (Kasatkin *et al.*, 2020a,b). It is also the case for biraite-group members (Fig. 8) where any *REE* heavier than Nd was below its EMPA detection limit and La and Ce are the main varying components at the *A* sites, while Pr and Nd, are strongly subordinate and do not exceed a total 0.31 apfu. The first scheme of isomorphic substitutions leads, therefore, to an extended solid-solution system including all the members of the group (Fig. 9). As was noted above, alexkuznetsovite-(La) and alexkuznetsovite-(Ce) co-exist in seven samples while compositions corresponding to both biraite-(La) and biraite-(Ce) were recorded in six others. The second scheme shows a large degree of isomorphic substitution between Mn and Fe at the *M* site resulting in two compositional fields: alexkuznetsovite with Mn > Fe and biraite with Fe > Mn (Fig. 10). We also observed an extended solid-solution system between all four members of the group. Alexkuznetsovite-(Ce) and biraite-(Ce) occur together in five samples, while alexkuznetsovite-(La) and biraite-(La) are in two. Two nodules contain three of four members (all three new minerals co-existing in one and both alexkuznetsovites with biraite-(Ce) – in the other), however, no nodule was found including all four members of the group.

The mineral assemblage described was formed during metasomatic processes, where primary bastnäsite-(La)/-(Ce) of probable alkaline pegmatitic origin (Pekov *et al.*, 2002) was replaced by various *REE*-bearing Ca-, Fe-, Mn- and/or Al-silicates. Hence, the composition of biraite-group minerals is influenced by *REE* distribution of the bastnäsite precursor, the chemical

https://doi.org/10.1180/mgm.2021.64 Published online by Cambridge University Press

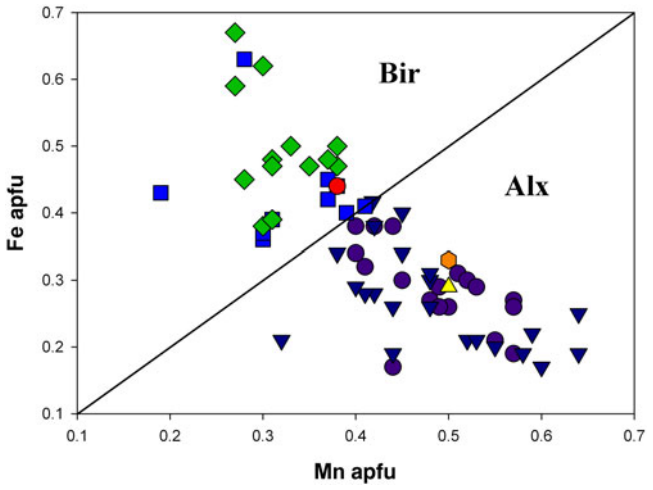

Fig. 10. Mn *vs*. Fe at the *M* site in minerals of the biraite group showing their distribution between alexkuznetsovite (Alx, Mn > Fe) and biraite (Bir, Fe > Mn) compositional fields. For legend see Fig. 9.

composition of the fluids and the crystal-chemical constraints of the co-crystallised minerals.

Supplementary material. To view supplementary material for this article, please visit: https://doi.org/10.1180/mgm.2021.64

Acknowledgements. We thank Dan Holtstam and an anonymous referee, Structures Editor Peter Leverett, Associate Editor Mihoko Hoshino and Principal Editor Stuart Mills for constructive comments that improved the quality of the manuscript. The interpretation of the Raman spectra was performed in accordance with the state task, state registration No. AAAA-A19-119092390076-7.

References

Belogub E.V., Krivovichev S.V., Pekov I.V., Kuznetsov A.M., Yapaskurt V.O., Kotlyarov V.A., Chukanov N.V. and Belakovskiy D.I. (2015) Nickelpicromerite, $K_2Ni(SO_4)_2{\cdot}6H_2O$, a new picromerite-group mineral from Slyudorudnik, South Urals, Russia. *Mineralogy and Petrology*, **109**, 143–152.

Britvin S.N., Dolivo-Dobrovolsky D.V. and Krzhizhanovskaya M.G. (2017) Software for processing the X-ray powder diffraction data obtained from the curved image plate detector of Rigaku RAXIS Rapid II diffractometer. *Zapiski Rossiiskogo Mineralogicheskogo Obshchestva*, **146**, 104–107 [in Russian].

Chukanov N.V. (2014) *Infrared Spectra of Mineral Species: Extended Library*. Springer-Verlag, Dordrecht, 1716 pp.

Chukanov N.V. and Chervonnyi A.D. (2016) *Infrared Spectroscopy of Minerals and Related Compounds*. Springer-Verlag, Cham, 1109 pp.

Gagné O.C. and Hawthorne F.C. (2015) Comprehensive derivation of bond-valence parameters for ion pairs involving oxygen. *Acta Crystallographica*, **B71**, 562–578.

Jentzsch P.V., Kampe B., Ciobotă V., Rösch P. and Popp J. (2013) Inorganic salts in atmospheric particulate matter: Raman spectroscopy as an analytical tool. *Spectrochimica Acta* A, **115**, 697–708.

Kagi H., Nagai T., Loveday J.S., Wada C. and Parise J.B. (2003): Pressure-induced phase transformation of kalicinite ($KHCO_3$) at 2.8 GPa and local structural changes around hydrogen atoms. *American Mineralogist*, **88**, 1446–1451.

Kasatkin A.V., Popov V.A., Kuznetsov A.M. and Nestola F. (2017) Dingdaohengite-(Ce) from Vishnevye Mountains (Southern Urals, Russia). *Mineralogiya*, **3**, 3–8 [in Russian with English abstract].

Kasatkin A.V., Škoda R. and Kuznetsov A.M. (2019a) Allanite-(Nd) of Sapfirinovaya pit, Southern Urals: first finding in Russia. *Mineralogiya*, **5** (1), 15–23 [in Russian with English abstract].

Kasatkin A.V., Škoda R., Nestola F., Kuznetsov A.M., Belogub E.V. and Agakhanov A.A. (2019b) Roentgenite-(Ce) and other *REE*-fluorcarbonates from the vein 35, Vyshnevye Mountains, Southern Urals. *Mineralogiya*, **5**, 10–22 [in Russian with English abstract].

Kasatkin A.V., Zubkova N.V., Pekov I.V., Chukanov N.V., Škoda R., Agakhanov A.A., Belakovskiy D.I. and Pushcharovsky D.Y. (2019c) Alexkuznetsovite-(La), IMA 2019–081. CNMNC Newsletter No. 52. *Mineralogical Magazine*, **83**, 887–893.

Kasatkin A.V., Zubkova N.V., Pekov I.V., Chukanov N.V., Škoda R., Polekhovsky Y.S., Agakhanov A.A., Belakovskiy D.I., Kuznetsov A.M., Britvin S.N. and Pushcharovsky D.Yu. (2020a): The mineralogy of the historical Mochalin Log *REE* deposit, South Urals, Russia. Part I. New gatelite-group minerals ferriperbøeite-(La), $(CaLa_3)(Fe^{3+}Al_2Fe^{2+})[Si_2O_7][SiO_4]_3O(OH)_2$, and perbøeite-(La), $(CaLa_3)(Al_3Fe^{2+})[Si_2O_7][SiO_4]_3O(OH)_2$. *Mineralogical Magazine*, **84**, 593–607.

Kasatkin A.V., Zubkova N.V., Pekov I.V., Chukanov N.V., Ksenofontov D.A., Agakhanov A.A., Belakovskiy D.I., Polekhovsky Yu.S., Kuznetsov A.M., Britvin S.N., Pushcharovsky D.Yu. and Nestola F. (2020b) The mineralogy of the historical Mochalin Log *REE* deposit, South Urals, Russia. Part II. Radekškodaite-(La), $(CaLa_5)(Al_4Fe^{2+})[Si_2O_7][SiO_4]_5O(OH)_3$, and radekškodaite-(Ce), $(CaCe_5)(Al_4Fe^{2+})[Si_2O_7][SiO_4]_5O(OH)_3$, two new minerals with a novel-type structure belonging to epidote–törnebohmite polysomatic series. *Mineralogical Magazine*, **84**, 839–853.

Kasatkin A.V., Zubkova N.V., Pekov I.V., Chukanov N.V., Škoda R., Agakhanov A.A., Belakovskiy D.I., Plášil J., Kuznetsov A.M., Britvin S.N. and Pushcharovsky D.Yu. (2020c) The mineralogy of the historical Mochalin Log *REE* deposit, South Urals, Russia. Part III. Percleveite-(La), $La_2Si_2O_7$, a new *REE* disilicate mineral. *Mineralogical Magazine*, **84**, 913–920.

Kasatkin A.V., Zubkova N.V., Pekov I.V., Chukanov N.V., Škoda R., Agakhanov A.A., Belakovskiy D.I. and Pushcharovsky D.Y. (2020d) Alexkuznetsovite-(Ce), IMA 2019–118. CNMNC Newsletter No. 54. *Mineralogical Magazine*, **84**, 359–365.

Kasatkin A.V., Zubkova N.V., Pekov I.V., Chukanov N.V., Škoda R., Agakhanov A.A., Belakovskiy D.I., Kuznetsov A.M. and Pushcharovsky D.Y. (2020e) Biraite-(La), IMA 2020–020. CNMNC Newsletter No.56; *Mineralogical Magazine*, **84**, 623–627.

Kolisnichenko S.V., Popov V.A., Epanchintsev S.G. and Kuznetsov A.M. (2017) *Mineraly Yuzhnogo Urala. Mineraly Chelyabinskoy Oblasti. Encyclopedia uralskogo kamnia [Minerals of Southern Urals. Minerals of Chelyabinsk district. Encyclopedia of the Urals stone]*. Chelyabinsk, Sanarka, Russia, 416 pp. [in Russian].

Konev A., Pasero M., Puscharovsky D., Merlino S., Kashaev A., Suvorova L., Ushchapovskaya Z., Nartova N., Lebedeva Y. and Chukanov N. (2005) Biraite-(Ce), $Ce_2Fe^{2+}(CO_3)(Si_2O_7)$, a new mineral from Siberia with a novel structure type. *European Journal of Mineralogy*, **17**, 715–721.

Mandarino J.A. (1981) The Gladstone-Dale relationship. IV. The compatibility concept and its 209 application. *The Canadian Mineralogist*, **41**, 989–1002.

McDonough W.F. and Sun S.-s. (1995) The composition of the Earth. *Chemical Geology*, **120**, 223–253.

Mills S.J., Hatert F., Nickel E.H. and Ferraris G. (2009) The standardisation of mineral group hierarchies: application to recent nomenclature proposals. *European Journal of Mineralogy*, **21**, 1073–1080.

Pekov I.V., Alimova A.N., Kononkova N.N. and Kanonerov A.A. (2002) On the mineralogy of Mochalin Log at Southern Urals I. Minerals of the bastnäsite family: history of studies and new data. *Uralskiy Geologicheskiy Zhournal* (*Uralian Geological Journal*), **4**(28), 127–144 [in Russian].

Pekov I.V., Zubkova N.V., Yapaskurt V.O., Belakovskiy D.I., Chukanov N.V., Kasatkin A.V., Kuznetsov A.M. and Pushcharovsky D.Y. (2013) Kobyashevite, $Cu_5(SO_4)_2(OH)_6{\cdot}4H_2O$, a new devilline-group mineral from the Vishnevye Mountains, South Urals, Russia. *Mineralogy and Petrology*, **107**, 201–210.

Rigaku (2018) *CrysAlisPro Software system, version 1.171.39.46*. Oxford Diffraction, UK.

Sheldrick G.M. (2015) Crystal structure refinement with SHELXL. *Acta Crystallographica*, **C71**, 3–8.

Warr L.N. (2021) IMA–CNMNC approved mineral symbols. *Mineralogical Magazine*, **85**, 291–320, http://dx.doi.org/10.1180/mgm.2021.43.